

P198

Electric Permittivity Hysteresis Measurements During Drainage and Imbibition of Salt Water in a Three-layer Sand

M. Kavian* (Delft University of Technology), E.C. Slob (Delft University of Technology) & W.A. Mulder (Delft University of Technology/Shell E&P)

SUMMARY

We measured the electric permittivity of a three-layer unconsolidated sand as a function of frequency, water saturation, and salinity. To ultimate objective is to determine if the effect of heterogeneities at scales much smaller than the skin depth can be captured by introducing effective frequency-dependent electrical values whose behaviour can be described by simple functions. We employ the parallel-plate capacitor technique to measure complex impedance for frequencies between 200 Hz and 3 MHz. We have conducted main drainage and secondary imbibition cycles for unconsolidated sand-saline water systems at atmospheric pressure and temperatures between 21°C and 22°C. We found hysteresis in electric permittivity, caused by redistribution of the water and air phases. The hysteresis effect becomes more pronounced at higher concentrations of salt. The possibility of replacing a layered structure by an effectively homogeneous medium to define its electric properties at all saturation levels is shown to depend on both frequency and salinity of the pore fluid. For some salinities and frequencies the measured electric property falls well within the Hashin-Strikman bounds, while for other, new models are necessary to describe the response.

Introduction

Maxwell's equations and Ohm's law describe the diffusion of electromagnetic fields in the earth. For diffusive electromagnetic field applications, the electric conductivity is usually taken to depend only on position and not on frequency. This implies that IP effects are ignored. The introduction of a complex-valued conductivity, with an imaginary part depending on frequency, allows the inclusion of IP effects.

We want to experimentally measure the electric behaviour of a layered medium as a function of water saturation and salinity for a wide range of frequencies. These dependencies are investigated for unconsolidated layered sands during imbibition, drainage, and secondary imbibition of water with different salinity levels. The key issue concerning the electrical behaviour is the electric hysteresis between the drainage and the secondary imbibition processes on a continuum scale. This implies that the electric response of a medium contains information about the pore fluid distributions in a heterogeneous porous medium.

Plug et al. (2007) have measured hysteresis in the real part of electric permittivity for homogeneous sand saturated with distilled water and showed that at a fixed optimally chosen frequency and for a given salinity the water saturation was a unique function of capillary pressure and electric permittivity. Laboratory experiments reported by Knight (1991) on sandstone show that measured values of electrical resistivity can depend on the saturation history of the sample. She found resistivity hysteresis between drainage and imbibition processes. Chelidze et al. (1999) have related this hysteric behaviour to the pore-scale fluid distribution during drainage and imbibition processes. We conducted the experiment for a layered model, using sands of different grain sizes and included one layer of clay in one of the experiments. The samples were sequentially saturated with water of three different salinities and the temperatures were kept between 21°C and 22°C.

Experimental setup

The sample holder, shown in Figure 1, is designed as a flat capacitor, similar to those used by Knight and Nur (1987) or Shen et al. (1987). The sample holder used here has an adjustable height. It consists of two parts: two porous plates act as electrodes (SIPERM R80, porous stainless steel), with a permeability of $3.3 \times 10^{-13} \text{ m}^2$ and a porosity of 0.33, and five PVC rings with a diameter of 15 cm and 3 cm height each containing the sample. To avoid leakage of water, we used O-rings in between the individual rings. These rings are mounted together with Teflon bolts at the top and bottom. A syringe pump (TELEDYNE ISCO pump, 1000D) was connected to the bottom of the sample holder and could be set to a constant injection or collection rate with an accuracy of $\pm 0.005 \text{ ml/h}$. The sample holder was put in a metallic box to shield it from external noise, see Figure 1.

A precision component analyzer (Wayne-Kerr, 6640A) was used to measure the impedance amplitude, $|Z|$ [Ω], and the phase angle, φ [rad], as a function of the frequency. These are related to the effective complex permittivity, ϵ^* , of the sample, defined by $\epsilon^* = \epsilon_R - i\epsilon_I$ or the effective complex electric conductivity $\sigma^* = i\omega\epsilon_0\epsilon^* = \sigma_R + i\sigma_I$, where ϵ_0 is the permittivity of vacuum and ω is the angular frequency, defined by $\omega = 2\pi f$. The indices R and I represent the real and imaginary part. These are related by $\sigma_R = \omega\epsilon_0\epsilon_I$, $\sigma_I = \omega\epsilon_0\epsilon_R$. We also define the effective complex electric resistivity, $\rho^* = \rho_R - i\rho_I$, which is the reciprocal of electric conductivity and is given by,

$$\rho_R = \frac{\sigma_R}{\sigma_R^2 + \sigma_I^2} = \frac{\epsilon_I}{\omega\epsilon_0(\epsilon_R^2 + \epsilon_I^2)}, \quad \rho_I = \frac{\sigma_I}{\sigma_R^2 + \sigma_I^2} = \frac{\epsilon_R}{\omega\epsilon_0(\epsilon_R^2 + \epsilon_I^2)}.$$

We are interested in the behaviour of these electric parameters as a function of frequency, water saturation, and salinity.

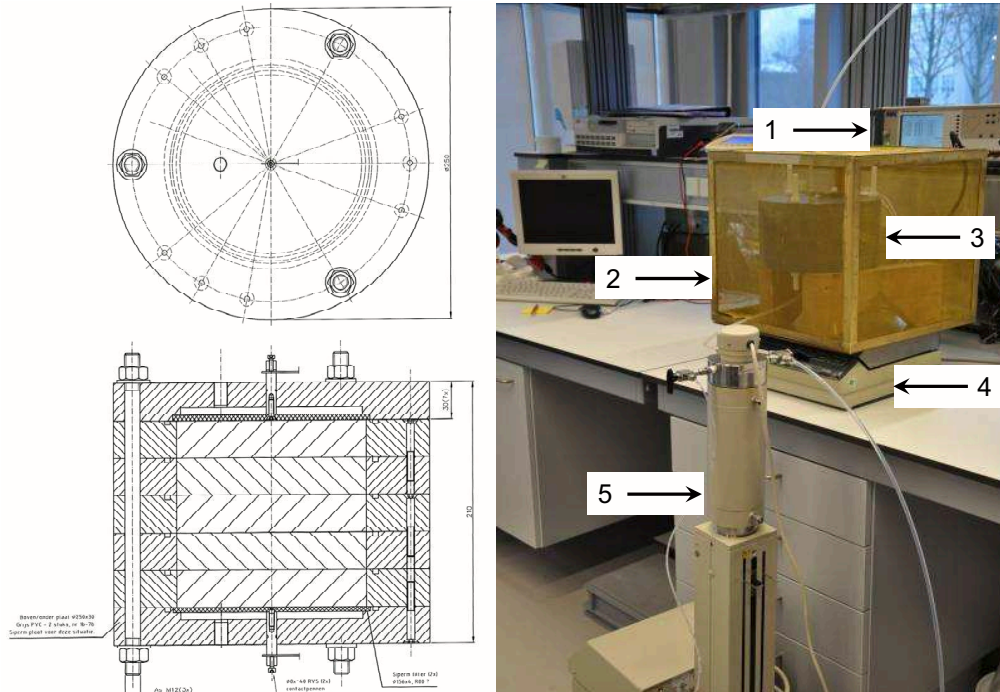


Figure 1: (Left) Schematic of the sample holder: top and front view; (right) experimental set up, 1. Component analyzer, 2. Faraday cage, 3. sample holder, 4. balance, 5. ISCO pump.

Experimental Procedure

We have used the experimental method for both the fine- and coarse-grained unconsolidated quartz sand samples, applying different degrees of saturation and three different concentrations of salt (0.001, 0.01, and 0.1 mol/lit). The coarse and fine sands have an average grain size fraction from 350 to 420 (D70) and 150 to 175 (D25) micron, respectively. The untreated sands, with a height of 9 cm and a diameter of 15 cm, were placed in the sample holder. We considered different combinations of a three-layer model and also two homogeneous cases with two different grain sizes of sand. The combinations used are sketched in Figure 2. Four different stacks of layers were constructed and the experiment was carried out for each of them. The sample holder was vibrated for 15 minutes to reach a porosity of 0.375 ± 0.005 and 0.395 ± 0.005 for the coarse- and fine-grain sands, respectively. Then the sample holder was put inside the Faraday cage and the sample holder was filled with the salt water in the lowest concentration of salt (primary imbibition) by injecting it from the bottom. In the next stage a constant water refill flow rate of 2 ml/min was applied using the ISCO pump (main drainage process) and this process was continued until the flow stopped when the pump did no longer overcome the capillary pressure to remove water from the

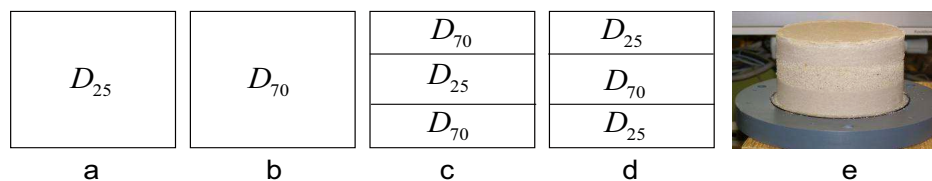


Figure 2: Four different configurations of the sand pack: (a) A homogeneous fine sand; (b) A homogeneous coarse sand; (c, d) Three layer sands with different grain size geometries; (e) Picture of the real three-layered sand sample. The height of each layer is 3 cm, the diameter is 15 cm, and the total height is 9 cm in each configuration.

sample. Then, the second imbibition process started with the pump set to the same constant injection flow rate.

Data Analysis

The complex capacitance is inversely proportional to the complex impedance $z^* [\Omega]$, by $C^* = \frac{1}{i\omega Z^*}$ and $Z^* = |Z|e^{i\varphi}$. The configuration is a parallel circuit, $C_{total}^* = C_{sample}^* + C_{residual}^*$, for which C_{total}^* is considered as the sum of the capacitance of the sample (C_{sample}^*) and the capacitance residual contributions ($C_{residual}^*$) of the other parts. We assume no change for this residual capacitance and subtract it from the total capacitance to obtain the complex relative electrical permittivity of the sample, $\epsilon_r^* = \left(\frac{1}{2\pi f} \cdot \frac{1}{iZ_{total}^*} - \frac{1}{2\pi f} \cdot \frac{1}{iZ_{residual}^*} + \frac{\epsilon_0 A}{d} \right) \cdot \frac{d}{\epsilon_0 A}$, $A [m^2]$ and $d [m]$ are the cross-sectional area and the height of the sample, respectively. The value of $Z_{residual}^*$ is obtained from air measurements. We obtain the water saturation from the produced or injected saline water volume during drainage or imbibition processes, respectively. This is done using a balance. We evaluated the dead volume of the water which exists between the SIPERM and the caps at the top and bottom of the sample holder by looking at the change of the impedance data versus time and knowing the saturation time and the saline water flow rate.

Experimental results and discussion

Figure 3 shows three plots of the real part of the electric permittivity versus water saturation at frequencies 105 KHz, 1.050 MHz, 2.1 MHz, and 3 MHz, in each plot for a single salt concentration. In Figure 3a, obtained at the lowest salinity with concentration of $C=1$ mmol/l, the drainage curves for frequencies above 1 MHz run almost in parallel and lie above the corresponding imbibition curves. The measured electric permittivities satisfy the Hashin-Shtrikman bounds for frequencies above 1 MHz and low salinities, implying that the system of layers can be considered as an effective medium or a macroscopically homogeneous mixture. Increasing the salinity by an order of magnitude at these high frequencies the medium is still an effective medium, but the drainage curves have all dropped below the imbibition curves indicating a change in capacitive effect of the unsaturated sands, as can be observed in Figure 3b. Increasing the salinity by another order of magnitude leads to strong hysteretic effect at high saturation levels up to at least 2 MHz, as can be seen in Figure 3c. At low frequency all models show clear hysteretic effect in their electric response as a function of drainage or imbibition, although the specific behaviour can be seen to depend on salinity.

Conclusions

The possibility of replacing a layered structure by an effectively homogeneous medium to define its electric properties has been shown to depend on frequency and salinity of the pore fluid. For some salinities and frequencies the measured electric property falls well within the Hashin-Shtrikman bounds, while for other new models are necessary to describe the response.

Acknowledgments

We thank H.K.J. Heller and F.C. Riem Vis for technical support and Delft Earth and Shell for funding the project.

References

Chelidze, T. L., Y. Gueguen, and C. Ruffet, 1999, Electrical spectroscopy of porous rocks: A review — II. Experimental results and interpretation: *Geophysical J. Intern.*, **137**, 16–34.

Knight, R. J., and A. Nur (1987), The dielectric constant of sandstones, 60 kHz to 4 MHz, *Geophysics*, **52**, 644–654.

Knight, R., 1991, Hysteresis in the electrical resistivity of partially saturated sandstones: *Geophysics*, **56**, 2139–2147.

Plug, W. J., E. C. Slob, J. Bruining, and L. M. Moreno Tirado (2007), Simultaneous measurement of hysteresis in capillary pressure and electric permittivity for multi-phase flow through porous media, *Geophysics*, **72**(3), A41–A45.

Shen, L. C., H. Marouni, Y. Zhang, and X. Shi (1987), Analysis of the parallel-disk sample holder for dielectric permittivity measurement, *IEEE TGRS*, **25**, 534–539.

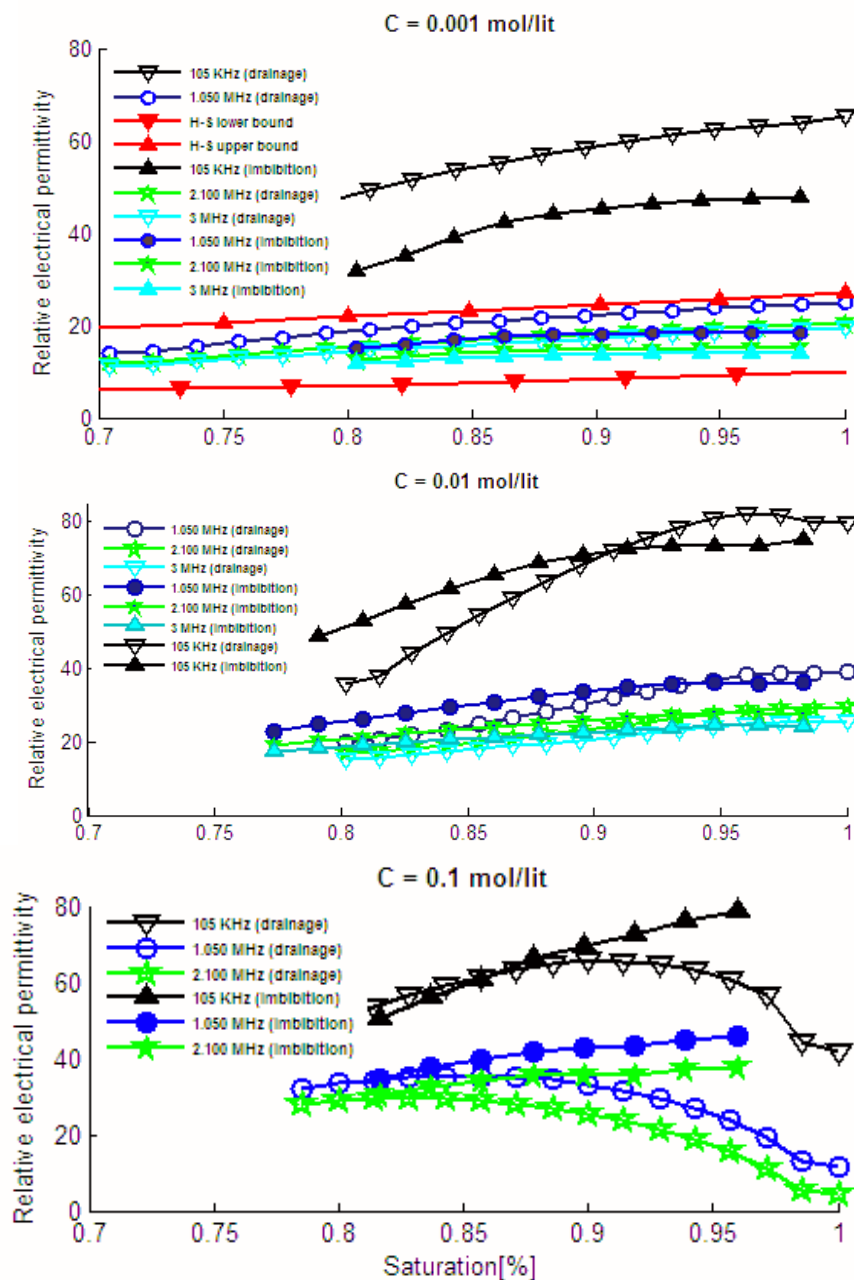


Figure 3: Drainage-imbibition hysteresis for a three-layer unconsolidated sand for three different salt concentrations; a. $C = 1$ mmol/l, b. $C = 10$ mmol/l, c. $C = 100$ mmol/l.